Target-Excitation Effects in Stripping Reactions*

F. S. LEVIN†
Brookhaven National Laboratory, Upton, New York
(Received 4 January 1966; revised manuscript received 8 March 1966)

Target-excitation effects are studied in (d,p) and (d,n) reactions using simple microscopic models. These effects occur when the outgoing nucleon excites the target nucleus; the stripped nucleon then couples with this excited state to form the final nuclear state. By choosing the optical potential for elastic scattering of the outgoing nucleon by the target nucleus in its ground state as the generator of the final-state distorted waves, and making the usual assumptions of the distorted-wave model, the distorted-wave amplitude separates into the standard distorted-wave Born-approximation amplitude plus one involving target excitation alone. Assuming a shell-model description of the target and residual nuclei and using two-body forces to describe the interaction between the outgoing nucleon and target nucleus, an angular-momentum decomposition of the target-excitation amplitude is made. Numerical estimates of the effect of target excitation are obtained using the following assumptions for the $Ca^{40}(d,p)Ca^{41}$ reaction: the deuteron is a point particle; the two-body force has a Gaussian shape; the target nucleus is doubly magic; the final nucleus is doubly magic plus one open shell; the single-particle states are harmonic-oscillator states; both the real and imaginary parts of the deuteron and proton optical potentials have a Saxon-Woods form factor (volume absorption). Results are obtained for various oscillator strengths and well parameters. Except for certain cases, the effects of target excitation are found to be small. Angular-correlation measurements are discussed as a possible means for detecting the presence of nonnegligible target-excitation effects.

I. INTRODUCTION

IN deriving the amplitude of the distorted-wave model of (d,p) reactions,[1] several terms are ignored, either on the expectation that they are small or because realistic calculations have so far not been feasible. We examine one term from the former class in the present work. This term is the matrix element of $V_{pt}-U_p$, where V_{pt} is the interaction between the outgoing proton and the target nucleus, and U_p is the complex potential well which generates the final-state proton-distorted wave function.[2] Other effects, due to inclusion of higher order terms in approximating the exact wave function, inclusion of first-order exchange effects, or inclusion of the matrix element of the imaginary part of U_p are not considered.

Our treatment of the (d,p) amplitude is standard in almost every respect (apart from studying the $V_{pt}-U_p$ matrix element) except in our choice of U_p. Any choice of U_p is permitted when the exact amplitude is considered, since the exact result is independent of U_p. This is not true of approximations. The *standard choice* of U_p is a complex well whose phase shifts reproduce the cross section for elastic scattering of the outgoing proton by the residual nucleus in its final state.[1] We choose instead, the complex well whose phase shifts fit the cross section for elastic scattering of the outgoing proton by the *target* nucleus in its *ground* state.

The main reason for this choice is one of practicality and is related to the fact that the parameters of the complex potential well are determined empirically. The difficulty of measuring proton elastic scattering by nuclei in excited states is evident. There is no guarantee that parameters determined from ground-state elastic scattering by the same nucleus, or by neighboring nuclei, as is now done, will always be correct. With our choice, and the usual approximations, all relevant elastic-scattering measurements are feasible. Our choice also leads to a slightly simpler approximate amplitude, as we shall see.

The above remarks are illustrated by a consideration of the general theory which we outline now. The exact amplitude T including exchange effects, can be written in the form

$$T=\langle k_p,J_fT_f|V_{np}+V_{pt}|\Psi^A\rangle, \tag{1}$$

where Ψ^A is the exact, antisymmetric scattering wave function (properly normalized), $|k_p\rangle$ is a proton plane wave, $|J_fT_f\rangle$ is the final state of the residual nucleus labeled by spin and isobaric spin (J_f,T_f) and V_{np} is the interaction between the outgoing proton p and the captured neutron n. Introducing the potential well U_p and the ingoing wave $|k_p^{(-)}\rangle$ in this well, Eq. (1) may be rewritten using the Gell-Mann and Goldberger theorem[3] as

$$T=\langle k_p^{(-)},J_fT_f|V_{np}+V_{pt}-U_p|\Psi^A\rangle. \tag{2}$$

Let $\{|J_tT_t\rangle\}$ denote the states of the target nucleus and $\{|\alpha_v\rangle\}$ denote the states of the deuteron, with specific labeling: the labels n and p are assumed to be in $|\alpha\rangle$ and the remainder are in $|J_tT_t\rangle$. Then

$$\Psi^A=\sum_{t,\alpha}|J_tT_t\rangle|\alpha\rangle\psi_{\alpha,t} \tag{3}$$

* Work performed under the auspices of U. S. Atomic Energy Commission.

† Present address: Theoretical Physics Division, Atomic Energy Research Establishment, Harwell, Berkshire, England.

[1] W. Tobocman, *Theory of Direct Nuclear Reactions* (Oxford University Press, London, 1961); N. Austern, in *Selected Topics in Nuclear Theory*, edited by F. Janouch (International Atomic Energy Association, Vienna, 1963); N. Glendenning, Ann. Rev. Nucl. Sci. **13**, 191 (1963); G. R. Satchler, Nucl. Phys. **55**, 1 (1964).

[2] Previous accounts of the early portions of this work were discussed in an unpublished manuscript (1963). See also F. S. Levin, Bull. Am. Phys. Soc. **9**, 446 (1964); **10**, 511 (1965).

[3] M. Gell-Mann and M. Goldberger, Phys. Rev. **91**, 398 (1953).

is a valid expansion for Ψ^A such that $\psi_{0,i}$ yields the complete elastic amplitude.[4] The states $|J_iT_i\rangle$ and $|\alpha=0\rangle$ denote the target and dueteron ground states, respectively.

The major approximation of the distorted-wave model is that within the matrix element of Eq. (2),

$$\Psi^A \approx |J_iT_i\rangle|\alpha=0\rangle\psi_{0,i}. \tag{A}$$

As discussed elsewhere,[4] approximation (A) leads to an amplitude in the case of elastic or inelastic scattering which contains second-, and higherorder exchange effects but no first-order exchange effects such as the analog of heavy-particle stripping.[5] As stated above, we make no attempts in the present work to include such first-order effects [see Eq. (4)] which are also not obtained from (A) and Eq. (4).

It is usual to assume further[1] that $\psi_{0,i}$ may be well represented by a function $|k_d^{(+)}\rangle$ generated by a complex well U_d such that $|k_d^{(+)}\rangle$ yields the observed elastic deuteron phase shifts. This is the second important approximation of the distorted-wave model. Making this assumption, we find that

$$T \approx T_{\mathrm{DW}} = \langle k_p^{(-)}, J_fT_f|\, V_{np} + V_{pt} - U_p|\, J_iT_i, \alpha=0, k_d^{(+)}\rangle. \tag{4}$$

Since (4) is only an approximation to T, it is clear that different choices of U_p may produce different amplitudes.

The third important assumption of the distorted-wave model is that $V_{pt}-U_p$ is sufficiently small that it is ignorable.[6] In the present work we assume instead that U_p is well approximated by its lowest order term:

$$U_p \approx \langle J_iT_i|\, V_{pt}|\, J_iT_i\rangle; \tag{B}$$

with assumption (B), U_p will now not cancel all of V_{pt}, as we shall see. As usual,[1] we ignore the imaginary term in U_p. It will be recalled that the lowest order approximation to the standard choice for U_p would lead not to (B) but to

$$U_p \approx \langle J_fT_f|\, V_{np}+V_{pt}|\, J_fT_f\rangle. \tag{B'}$$

To use (B), we introduce the fractional-parentage expansion of $|J_fT_f\rangle$ into states of the target plus single-particle states of the captured neutron:

$$|J_fT_f\rangle = \sum_{t,n} A_{t,n}(f)\,|\,J_tT_t\rangle|\,j_n\tfrac{1}{2}\rangle, \tag{5}$$

where $A_{t,n}$ is a product of fractional-parentage coefficient and Wigner coefficients and $(j_n,\frac{1}{2})$ are the spin and isobaric spin of the captured neutron. The subscript t runs over the values $t=i$ (ground state) and $t=e$ (excited states).

If Eq. (5) is now substituted into Eq. (4), *(B) may be used to eliminate the matrix elements of V_{pt} diagonal in the states of the target nucleus.* The resulting expression for T_{DW} is

$$\begin{aligned} T_{\mathrm{DW}} &= \sum_n A_{i,n}(f)\langle k_p^{(-)}, j_n\tfrac{1}{2}|\, V_{np}|\alpha=0, k_d^{(+)}\rangle \\ &\quad + \sum_{n,e} A_{e,n}(f)\langle k_p^{(-)}, j_n\tfrac{1}{2}|\, \mathcal{U}_p(e,i)|\alpha=0, k_d^{(+)}\rangle, \\ &\equiv T_{\mathrm{DWBA}} + T_{\mathrm{EXC}}, \end{aligned} \tag{6}$$

where

$$\mathcal{U}_p(e,i) = \langle J_eT_e|\, V_{pt}|\, J_iT_i\rangle. \tag{7}$$

The term in T_{DW} involving V_{np} is the familiar distorted-wave Born-approximation (d,p) amplitude, denoted here by T_{DWBA}. It is diagonal in the states of the target nucleus and corresponds to formation of $|J_fT_f\rangle$ by adding a neutron to the ground state of the target. The second term in T_{DW}, involving $\mathcal{U}_p(e,i)$, contains the new effect that we examine in the remainder of this paper. This new amplitude T_{EXC} corresponds to formation of the final state by coupling the neutron to an excited state (and only to an excited state) of the target. The target is excited by the interaction of the outgoing proton with the target nucleus. In shell-model language, the states $|J_eT_e\rangle$ are those obtained by angular-momentum recouplings within a shell or else by promotion of a single nucleon to an unoccupied j shell, since we shall assume that V_{pt} is given by a sum of two-body interactions.

If we had used assumption (B') rather than (B), we would have obtained an equation for T_{DW} that was the sum of the right-hand side of (6) plus an additional term diagonal in V_{pt}; i.e., a term $\langle J_iT_i|\, V_{pt}|\, J_iT_i\rangle$ would have made an extra contribution to T_{DWBA}.

Our concern is with evaluating T_{EXC} and comparing it with T_{DWBA}. We thus have to translate the schematic form of (6) into matrix elements with specific magnetic quantum numbers. This in turn means that we must specify the states $|J_fT_f\rangle$, $|J_eT_e\rangle$, and $|J_iT_i\rangle$ (i.e., the nuclear model) and thus the quantities $A_{t,n}(f)$, and also choose a form of V_{pt}. In the remainder of this paper we carry out this program.

II. THEORY

A. Angular-Momentum Expansion

In this section, we outline the steps required to express T_{EXC} as an expansion in angular-momentum quantum numbers. Detailed formulas for T_{EXC} for the case of arbitrary target nuclei are not presented since, on the one hand, such expressions are rather unwieldy,

[4] This expansion has been discussed for the cases of nucleon-nucleus and deuteron-nucleus elastic and inelastic scattering: F. S. Levin, Phys. Rev. **140**, 1099 (1965).

[5] For discussion of exchange effects in (d,p) reactions, see D. Robson, Proc. Phys. Soc. (London) **80**, 1067 (1962); Nucl. Phys. **33**, 594 (1962); **42**, 592 (1963); F. S. Levin, *ibid.* **36**, 119 (1962); L. Rodberg, *ibid.* **47**, 1 (1963); S. Edwards, *ibid.* **47**, 652 (1963). In spite of the large literature on exchange effects in direct reactions (much of it referred to in the above references), no satisfactory general treatment of the problem has yet been given. The role of exchange effects has remained one of the major mysteries of nuclear reaction theory.

[6] An exception is to be found in the work of Glendenning (Ref. 1), whose treatment is quite similar to ours.

while on the other hand, we consider only a greatly simplifying special case for our calculations. Instead, we provide enough details for the interested reader to be able to derive the formulas of the general case or the special case of Sec. II-C for himself. The various assumptions concerning nuclear structure, the form of the interaction V_{pt}, etc., are indicated. Since we include the effects of *closed* shells in evaluating T_{EXC}, and since we need not only parent but grandparent states (unlike the case of ordinary stripping) to evaluate reduced matrix elements, we discuss at some length the shell-model wave functions and the generalized coefficients of fractional parentage (cfp's) that have been used in the calculations. Although similar discussions have often been given, we include the present one as an aid to understanding the few formulas we do give and because they help to emphasize the important role played by hole states, i.e., core-excited states. A further point is that the generalized cfp's are not the familiar ones of the standard shell-model calculation. Finally, the discussion given, plus the material in the Appendix, should help to make this work reasonably self-contained.

We begin by rewriting Eq. (4) in a form which displays the relevant magnetic quantum numbers. Thus, $|JT\rangle \rightarrow |JM,TM_T\rangle$ and the state $|\alpha=0\rangle$ of the deuteron becomes $|1M_d,00\rangle$ with the second pair of numbers referring to isobaric spin. Equation (4) becomes in this notation

$$T_{\mathrm{DW}}=\langle k_p{}^{(-)}|\langle \tfrac{1}{2}\sigma_p,\tfrac{1}{2}\tau_p|\langle J_fM_f,T_fM_{T_f}|V_{np} +V_{pt}-U_p|J_iM_i,T_iM_{T_i}\rangle|1M_d,00\rangle|k_d{}^{(+)}\rangle, \quad (8)$$

where $|\frac{1}{2}\sigma_p,\frac{1}{2}\tau_p\rangle$ is the spin, isobaric-spin state of the proton.[7]

We now must specify the initial and final nuclear states so as to be able to use Eq. (5) and approximation (B). Since our purpose in this work is to obtain an estimate of the relative size of T_{EXC}, and not to fit particular data, we choose the simplest of nuclear models: the spherical shell model. For simplicity, we assume that the $|J_fT_f\rangle$ and $|J_iT_i\rangle$ may be well represented by a mixture of those configurations in which no more than two different j shells are unfilled. This restriction may be dropped, but the formulas become rather cumbersome; the case of two unfilled shells is sufficiently illustrative for our purposes. As an example, we consider the final state $|J_fM_f,T_fM_{T_f}\rangle$ whose general form is given by

$$|J_fM_f,T_fM_{T_f}\rangle = \sum_{\substack{n \\ a+b=\mathcal{O}+1}} B_n[j'^a(J_n'T_n'\alpha_n')j''^b(J_n''T_n''\alpha_n'')] \times|\prod_{j_c} j_c{}^{4j_c+2}(00)j'^a(J_n'T_n'\alpha_n') \times j''^b(J_n''T_n''\alpha_n''); J_fM_f,T_fM_{T_f}\rangle. \quad (9)$$

The notation of Eq. (9) is as follows. The quantities a and b denote the number of nucleons in the open shells j' and j'', respectively ($\mathcal{O}$ is the number of open shell nucleons in $|J_iT_i\rangle$) and $j'^a(J_n'T_n'\alpha_n')$ are the quantum numbers of the group of nucleons of spin j'. A subscript n is included to account for the various possible spins and isobaric spins that are allowed for the configuration $(j')^a$; α denotes additional quantum numbers, such as seniority. The symbol j_c represents a closed-shell angular momentum. There can be $4j_c+2$ nucleons in a closed shell, with resulting $(JT)=(00)$. The numbers $B_n[\ ]$ are the various configuration strengths obtained, in general, from a shell-model analysis of energy-level spectra. Finally, J_n' and J_n'' are to be coupled to form J_f, etc.

Equation (5) represents the first type of fractional-parentage expansion we need to evaluate T_{DW}. To determine such an expansion for Eq. (9), we need the generalized cfp's for removing a particle from one of the states in (9), which contains identical, but inequivalent, nucleons. Let us consider one such state. Conforming to the standard convention, we remove the last particle, which is always taken to be the stripped nucleon. It is evident that this nucleon may come from the group j''^b, j'^a, or any closed shell, and further, we note that when a nucleon in group j is removed, none of the other groups are disturbed. Hence, the generalized cfp for removal of a nucleon having angular momentum j while leaving the remaining group of nucleons undisturbed is closely related to the ordinary cfp for removal of one nucleon from the usual configuration j^n. However, the requirement that the separated nucleon be the last nucleon regardless of its angular momentum, means that Racah coefficients appear as factors in the expression for the generalized cfp's, as we discuss in the Appendix.[8]

As an example of the equation that results on making such a fractional-parentage expansion, we exhibit the portion describing the removal of a nucleon in state $|j'\frac{1}{2}\rangle$ (we partially suppress magnetic quantum numbers):

$$|\prod_{j_c} j_c{}^{4j_c+2}(00)j'^a(J_n'T_n'\alpha_n')j''^b(J_n''T_n''\alpha_n''); J_fT_f\rangle = \sum_{\substack{J_2T_2\alpha_2 \\ JT_\alpha}} C(Jj'J_f;Mm'M_f)C(T\tfrac{1}{2}T_f;M_T\tau'M_{T_f})([j'^{a-1}(J_2T_2\alpha_2)j''^b(J_n''T_n''\alpha_n'')](JT\alpha),j'[\![J_fT_f) \times|j'^{a-1}(J_2T_2\alpha_2)j''^b(J_n''T_n''\alpha_n''); JM,TM_T\rangle|j'm',\tfrac{1}{2}\tau'\rangle+\cdots. \quad (10)$$

[7] By leaving τ_p unspecified, we can also include (d,n) reactions in our treatment.

[8] The generalized cfp's were first brought to the author's attention by D. Amit (private communication). A discussion similar to that of the Appendix is given by D. Amit and A. Katz, Nucl. Phys. 58, 388 (1964), although the generalized cfp's for hole states are not treated by these authors.

The closed shells are not explicitly included since they are not disturbed; the fact that they are considered is indicated by the normalization of the (⟦)'s, as discussed in the Appendix. For that portion of Eq. (10) describing the removal of the last nucleon from a closed-shell state, the generalized cfp is

$$(\{[j'^a(J_n'T_n'\alpha_n')j''^b(J_n''T_n''\alpha_n'')](J_fT_f)j_c^{+4j_c+1}(j_c\tfrac{1}{2})\}(JT\alpha),j_c⟦J_fT_f⟧),$$

and only a summation on $JT\alpha$ is needed since the $4j_c+1$ particles couple to the unique value of $(j_c\frac{1}{2})$. From these examples, it is evident that a shorthand notation for cfp's and the nuclear states would be convenient. The following is used: for an open shell cfp such as appears in Eq. (10) we write $([J_2T_2\alpha_2](JT\alpha), j_0⟦J_fT_f⟧)$, while for the closed shell cfp, we employ $(\{[n,a,b](J_fT_f)\}(JT), j_c⟦J_fT_f⟧)$. The nuclear states $|JT\rangle$ are labeled in the same way as the cfp's.

Substitution of (10) into (9), and (9) into (8) will then lead to a detailed expansion of T_{DW} similar to Eq. (6). However, we shall only consider the T_{EXC} part of T_{DW} in this section, since formulas for T_{DWBA} have been given in many places.[1] Since only states $|J_eT_e\rangle$ can occur in the expansion of $|J_fT_f\rangle$, we must omit those configurations (with proper strength) that are present in $|J_iT_i\rangle$. We indicate this symbolically by placing a prime on the coefficients $B_n[\ ]$.

Carrying out the relevant substitutions and using approximation (B), the T_{EXC} part of T_{DW} becomes

$$\begin{aligned}T_{\mathrm{EXC}}=\sum_{\substack{n\\ a+b=\mathcal{O}+1}} B_n'[a,b]\sum_{\substack{J_eT_e\alpha_e\\ M_eM_{T_e}\tau_n}} C(T_e\tfrac{1}{2}T_f;M_{T_e}\tau_nM_{T_f})\\ \times\{\sum_{\substack{J_2T_2\alpha_2\\ j_0m_n}} C(J_ej_0J_f;M_em_nM_f)([J_2T_2\alpha_2](J_eT_e\alpha_e),j_0⟦J_fT_f⟧)\\ \times\langle k_p^{(-)}|\langle\tfrac{1}{2}\sigma_p,\tfrac{1}{2}\tau_p|\langle j_0m_n,\tfrac{1}{2}\tau_n|\mathcal{V}_{J_eT_e}{}^o|k_d^{(+)}\rangle|1M_d,00\rangle\\ +\sum_{j_cm_n} C(J_ej_cJ_f;M_em_nM_f)(\{[n,a,b](J_fT_f)\}(J_eT_e\alpha_e),j_c⟦J_fT_f⟧)\\ \times\langle k_p^{(-)}|\langle\tfrac{1}{2}\sigma_p,\tfrac{1}{2}\sigma_p|\langle j_cm_n,\tfrac{1}{2}\tau_n|\mathcal{V}_{J_eT_e}{}^c|k_d^{(+)}\rangle|1M_d,00\rangle\}, \quad (11)\end{aligned}$$

where the coefficients B_n' are also written in an obvious shorthand and $C(abc;\alpha\beta\gamma)$ is a Wigner coefficient in the notation of Rose.[9] The labels o and c refer to open and closed shells, respectively. The effective interactions $\mathcal{V}_{J_eT_e}{}^o$ and $\mathcal{V}_{J_eT_e}{}^c$ are defined by

$$\mathcal{V}_{J_eT_e}{}^o=\langle[J_2T_2\alpha_2];J_eT_e|V_{pt}|J_iT_i\rangle$$

and

$$\mathcal{V}_{J_eT_e}{}^c=\langle[n,a,b](J_fT_f);J_eT_e|V_{pt}|J_iT_i\rangle,$$

with the dependence on (J_iT_i), any intermediate-state quantum numbers, and magnetic quantum numbers suppressed.

A more tractable expression may be obtained by expanding the deuteron wave function into spin and isobaric-spin components:

$$\begin{aligned}&|1M_d,00\rangle\\ &=|l=0\rangle 2^{-1/2}\sum_{\tau_p'\sigma_p'\sigma_n'}(-1)^{\frac{1}{2}-\tau_p'}C(\tfrac{1}{2}\,\tfrac{1}{2}\,1;\sigma_n'\sigma_p'M_d)\\ &\quad\times|\tfrac{1}{2}\tau_p'\rangle|\tfrac{1}{2}-\tau_p'\rangle|\tfrac{1}{2}\sigma_n'\rangle|\tfrac{1}{2}\sigma_p'\rangle, \quad (12)\end{aligned}$$

where $|l=0\rangle$ is the S-state portion of the deuteron ground state. Because of an approximation we make later, it is not necessary to consider the deuteron D state, although its inclusion is straightforward. Substitution of Eq. (12) into Eq. (11) and evaluation of the isobaric-spin scalar product for the captured nucleon then leads to an expression from which we define the effective proton interaction $\mathcal{U}_{J_eT_e}$:

$$\begin{aligned}\mathcal{U}_{J_eT_e}=\sum_{\tau_p'M_{T_e}}(-1)^{\frac{1}{2}-\tau_p'}C(T_e\tfrac{1}{2}T_f;M_{T_e}-\tau_p'M_{T_f})\\ \times\langle\tfrac{1}{2}\tau_p|\langle\tfrac{1}{2}\sigma_p|\mathcal{V}_{J_eT_e}|\tfrac{1}{2}\tau_p'\rangle|\tfrac{1}{2}\sigma_p'\rangle, \quad (13)\end{aligned}$$

where we have dropped superscripts.

The next step is to reduce the effective interaction $\mathcal{V}_{J_eT_e}$ to a more tractable form. To do so, we assume that the interaction V_{pt} may be adequately represented by a sum of two-body central forces. Spin-dependent forces could be included, as could three-body forces, but our aim is to obtain an estimate of the size of T_{EXC}. It is sufficient to use central forces to do this. (Similarly, in generating the distorted-waves $|k_p^{(-)}\rangle$ and $|k_d^{(+)}\rangle$, we shall take the complex wells to be spin-independent.) We thus assume that

$$\begin{aligned}V_{pt}=\sum_{\substack{\alpha\in\text{target}\\ \text{nucleus}}}V(\mathbf{r}_{p\alpha})\\ \times[A_W+A_BP_{p\alpha}{}^\sigma-A_HP_{p\alpha}{}^\tau+A_MP_{p\alpha}{}^x], \quad (14)\end{aligned}$$

where the P's are the usual exchange operators with coefficients normalized to unity.

We next expand the two-body interaction into multipoles in the usual way,

$$V(\mathbf{r}_{p\alpha})=\sum_{k\mu}v_k(r_p,r_\alpha)Y_k{}^\mu(\Omega_\alpha)Y_k{}^{\mu*}(\Omega_p). \quad (15)$$

[9] M. E. Rose, *Elementary Theory of Angular Momentum* (John Wiley and Sons, Inc., New York, 1957).

On substituting Eqs. (14) and (15) into (13), writing the exchange operators in the spherical basis and using the Wigner-Eckhart theorem[9] we may express $\mathfrak{U}_{J_eT_e}$ in terms of Wigner coefficients and reduced matrix elements. The reduced matrix elements may be evaluated in the standard way[10] in terms of various recoupling coefficients and generalized cfp's for grandparent states; we shall not, however, state the results here. It is sufficient to note that, in general, the resulting expressions involve many restricted sums on angular momenta, in contrast to the simpler case of T_{DWBA}. These sums generally do *not* have closed-form expressions. There is also a dependence of $\mathfrak{U}_{J_eT_e}$ on the radial part of the effective interaction $V_{lkl'}(r_p)$ given by

$$V_{lkl'}(r_p)=\int dr\, r^2\varphi_l(r)v_k(r_p,r)\varphi_{l'}(r)\,. \qquad (16)$$

In Eq. (16), φ_l is a bound-state shell-model wave function of angular-momentum l and is assumed to be independent of $j(=l\pm\frac{1}{2})$. The principal quantum-number dependence in φ_l is suppressed. The subscript k in (16) is the multipolarity from Eq. (15).

In evaluating $\mathfrak{U}_{J_eT_e}$ in terms of Wigner coefficients, etc., we also obtain the isobaric-spin dependence. A simple calculation then suffices to show that T_{EXC} has the same isobaric-spin dependence as T_{DWBA}, viz., $C(T_i\tfrac{1}{2}T_f; M_{T_i}-\tau_pM_{T_f})$.

It is evident that the k dependence of $\mathfrak{U}_{J_eT_e}$ will be restricted because of the assumption that $|J_eT_e\rangle$ and $|J_fT_f\rangle$ are described in terms of the shell model. A further restriction arises, however, because the nucleon p is only allowed to interact with the open-shell nucleons of $|J_eT_e\rangle$, while the nucleon in $|J_iT_i\rangle$ must be an open-(closed)-shell nucleon as j_n is an open- (closed)-shell angular momentum, where j_n is the angular momentum of the captured neutron.

To see this, we first remark that because of the antisymmetry of $|J_eT_e\rangle$ and $|J_iT_i\rangle$, $\sum_\alpha v_k(r_\alpha,r_p)\rightarrow Av_k(r_A,r_p)$, where A is the number of nucleons in the target (also, it is the label for the last target nucleon). Next, in order to evaluate the reduced matrix elements, it is necessary to expand both $|J_eT_e\rangle$ and $|J_iT_i\rangle$ via single-particle cfp's; the resulting core states are grandparent states for $|J_fT_f\rangle$. The reduced matrix elements then become a sum of products of a single-particle reduced matrix element and a scalar product of two grandparent states; a nonvanishing result is obtained only if the grandparent states are identical. Let us now suppose j_n to be an open-shell angular momentum. Then $|J_eT_e\rangle$ and $|J_iT_i\rangle$ both have identical closed-shell structures, and a nonzero overlap among grandparent states will occur only if nucleon A comes from an open shell in both $|J_eT_e\rangle$ and $|J_iT_i\rangle$. On the other hand, if j_n is a closed-shell angular momentum, then $|J_eT_e\rangle$ has one more hole state and one more open-shell state than $|J_iT_i\rangle$. A nonzero scalar product now occurs only if (a) an open-shell nucleon is removed from $|J_eT_e\rangle$, (b) the same hole state is created in the $|J_iT_i\rangle$ parent as in $|J_eT_e\rangle$, *and* (c) the remaining open-shell nucleons in the $|J_eT_e\rangle$ parent state couple to form $|J_iT_i\rangle$.

An interesting consequence of the above rules is that for those reactions where T_{DWBA} vanishes because $|J_iT_i\rangle$ is not a parent for $|J_fT_f\rangle$ [e.g., $B^{10}(d,\dot{p})B_{2.14}{}^{11*}$], j_n can take on only open-shell values. This follows from the fact that if j_n is a closed-shell angular momentum, then the open-shell nucleons in the $|J_fT_f\rangle$ grandparent state must couple to form $|J_iT_i\rangle$, but this is impossible by hypothesis.

Once $\mathfrak{U}_{J_eT_e}$ has been expressed in terms of the $V_{lkl'}$ and has been substituted into T_{EXC}, the remaining radial integrals can then be attempted. There are two such three-dimensional integrals to carry out: on the neutron ($\mathbf{r}_n$) and on the proton ($\mathbf{r}_p$) spatial coordinates. In order to do this, the deuteron internal wave function $\langle r_{np}|l=0\rangle$ must be expanded in terms of $\mathbf{r}_n$ and $\mathbf{r}_p$. The resulting expressions involve many coherent sums on angular momenta and an infinite sum of double integrals. These are rather complex to carry out because the deuteron center-of-mass state $\langle(\mathbf{r}_n+\mathbf{r}_p)/2|k_d{}^{(+)}\rangle$ will also have to the expanded in terms of $\mathbf{r}_n$ and $\mathbf{r}_p$. To simplify the calculations, we now assume that the deuteron ground state may be adequately represented, for the purposes of our calculation, by a delta function:

$$\langle\mathbf{r}_{np}|l=0\rangle\approx(4\pi)^{1/2}N_d\alpha^{-2}\delta(\mathbf{r}_n-\mathbf{r}_p)\,, \qquad (C)$$

where the normalization is determined by requiring equality of the volume integrals of each side of (C). Except for normalization, use of (C) in T_{DWBA} produces the same matrix element as the standard zero-range approximation given by $\langle\mathbf{r}_{np}|V_{np}|l=0\rangle\approx-(\hbar^2/M)\times(4\pi)^{1/2}N_d\delta(\mathbf{r}_n-\mathbf{r}_p)$. Here, N_d is the deuteron normalization factor and α^{-1} is the size of the deuteron: $\alpha^{-1}\approx4.3$ f. One effect of (C) in T_{DWBA} will be to produce a factor $V_{np}(r_{np}=0)$, *and by choosing* $V_{np}=V(r_{np})$ *to have the same functional form as* $V(r_{p\alpha})$ *in Eq. (15), we shall be able to compare* T_{EXC} *and* T_{DWBA} *directly.*

We believe that the effect on T_{EXC} of approximation (C) will be twofold. First, it should produce a sharpening of the diffraction peaks of the angular distribution because the angular dependence of T_{EXC} will now be concentrated in a sum of terms similar to those of T_{DWBA}, rather than in an infinite sum of terms in which the $\mathbf{r}_n$ and $\mathbf{r}_p$ integrals tend to smear out the angular dependence because of the finite size of the deuteron. Secondly, we expect that now T_{EXC} will represent an upper bound to the result obtained if (C) were not used. This remark is based on plane-wave calculations[11] which showed that use of (C) increased the cross section over the result when (C) was not used. We do not expect that the use of distorted waves instead of plane waves should

[10] I. Talmi and A. de-Shalit, *Nuclear Shell Theory* (Academic Press Inc., New York, 1963).

[11] F. S. Levin (unpublished). Further comments are given in the next section.

alter this result. Hence, use of (C) is reasonable in that it allows us to bound the magnitude of $T_{\rm EXC}$, even though the angular distributions may not be too accurate.

The result of using (C) in $T_{\rm EXC}$ is to simplify the angular-momentum sums slightly and also to permit $T_{\rm EXC}$ to be put into a form resembling $T_{\rm DWBA}$. The general expression for $T_{\rm DW}$ is now

$$T_{\rm DW}=(2\pi)^{1/2}N_d\alpha^{-2}(-)^{\frac{1}{2}-\tau_p}C(T_i\tfrac{1}{2}T_f;\,M_{T_i}-\tau_pM_{T_f})\times\sum_{\substack{J_1J_2\lambda\\M_1M_2m}}C(\tfrac{1}{2}J_21;\,\sigma_pM_2M_d)C(J_iJ_1J_f;\,M_iM_1M_f)\times C(\lambda J_2J_1;\,mM_2M_1)[B_\lambda{}^m+B_\lambda{}^m(J_1J_2)]. \quad (17)$$

B. Properties of the Amplitude

We now examine the amplitude $T_{\rm DW}$. In (17), $B_\lambda{}^m$ is the angular-dependent factor of the usual stripping matrix element $T_{\rm DWBA}$. It contains the spectroscopic factor, reduced width, radial integrals, etc., and λ labels the transferred angular momentum. Also, $B_\lambda{}^m$ contains the factors $\delta_{\frac{1}{2}J_2}$ and $\delta_{j_nJ_1}$, i.e., no spin-flip terms occur and only the angular momentum of the captured neutron j_n couples with J_i to form J_f.

The amplitude $T_{\rm EXC}$ is given by that portion of Eq. (17) containing the factor $B_\lambda{}^m(J_1J_2)$. Each term $B_\lambda{}^m(J_1J_2)$ is given as a sum on numerous angular-momentum labels and involves the $B_n'[a,b]$ of Eq. (9), the generalized cfp's of Eq. (10), various recoupling coefficients, and radial integrals with the factors $V_{lkl'}$ as integrands. All magnetic quantum numbers have been removed from the $B_\lambda{}^m(J_1J_2)$, for which it may be shown that J_2 may be either $\frac{1}{2}$ or $\frac{3}{2}$, the latter corresponding to spin-flip processes due to the spin-exchange operator P^σ. Furthermore, since j_n couples with J_e to form J_f, and J_e and J_i are linked via the multipoles of the two-body interaction, then J_f and J_i can be linked by angular-momentum values other than j_n, as indicated by the J_1 sum in $B_\lambda{}^m(J_1J_2)$. A restriction on the coherency of like values of λ in $T_{\rm DWBA}$ and $T_{\rm EXC}$ thus follows: equal values of λ in $T_{\rm DWBA}$ and $T_{\rm EXC}$ are coherent only when $J_2=\frac{1}{2}$ and $J_1=j_0$ in $T_{\rm EXC}$. The other values of J_1 and J_2 will add incoherently with each other and with $T_{\rm DWBA}$.

These latter comments become obvious when the differential cross-section formula is written out:

$$\frac{d\sigma}{d\Omega}=\frac{\mu_p\mu_n}{(2\pi\hbar^2)^2}\frac{k_p}{k_d}[(2\pi)^{1/2}N_dC(T_i\tfrac{1}{2}T_f;\,M_{T_i}-\tau_pM_{T_f})]^2\times\frac{2J_f+1}{2J_i+1}\sum_{J_1J_2\lambda m}[(2J_2+1)(2\lambda+1)]^{-1}\times|B_\lambda{}^m+B_\lambda{}^m(J_1J_2)|^2.$$

A few further remarks may be made concerning the properties of $T_{\rm EXC}$. A well-known feature of $T_{\rm DWBA}$ is that only $|J_iT_i\rangle$ is allowed as a parent state, implying that λ takes on the open-shell value or values that give rise to the Butler stripping patterns. However, this is not true in $T_{\rm EXC}$ for two reasons. First, $|J_eT_e\rangle$ may contain configurations not occurring in $|J_iT_i\rangle$, and second, j_n can assume all possible closed-shell values because of the Pauli principle. As a specific example of which we make use later, consider $Ca^{40}(d,p)Ca^{41}$ (ground state, g.s.) and assume Ca^{40} to consist entirely of closed shells and Ca^{41}(g.s.) to contain these configurations plus an $f_{7/2}$ neutron. Then in $T_{\rm DWBA}$, $l_n=3$, but in $T_{\rm EXC}$ one finds $l_n=0$, 1, and 2, corresponding to the Ca^{40} configurations $s^{-1}f$, $p^{-1}f$, and $d^{-1}f$. The value $l_n=3$ in $T_{\rm EXC}$ is not allowed since only Ca^{40}(g.s.) is obtained from the closed-shell configuration and Ca^{40}(g.s.) by hypothesis cannot be a parent state in $T_{\rm EXC}$.

In general, not all the J_eT_e states are necessarily found in $T_{\rm EXC}$ for each j_n value, since the selection rule $\mathbf{J}_f=\mathbf{J}_e+\mathbf{j}_n$ must be satisfied. We may also write this as

$$\min|J_e\pm J_f\pm\tfrac{1}{2}|\leq l_n\leq J_e+J_f+\tfrac{1}{2}$$

in analogy to the similar form of the selection rule $\Delta(J_iJ_fj_n)$ for $T_{\rm DWBA}$. The parity selection rule $\pi_{J_f}=(-1)^{l_n}\pi_{J_e}$ is also obeyed, but because of core excitation it does not limit l_n as in the case of $T_{\rm DWBA}$.

In addition to the above rules, there are three others which we now summarize:

(1) If the "parity" of $T_{\rm DWBA}$ is defined as $(-1)^{l_n}$, then in $T_{\rm EXC}$ the only allowed λ values are those such that the parity of all matrix elements in $T_{\rm EXC}$ is $(-1)^\lambda=(-1)^{l_n}$.

(2) When j_n takes on closed-shell values in $T_{\rm EXC}$, only those states $|J_eT_e\rangle$ are allowed in which the open-shell nucleons have the quantum numbers of the initial state of the target nucleus.

(3) For the cases where $T_{\rm DWBA}=0$ because of failure to satisfy the triangle relation $\Delta(J_iJ_fj_n)$, the values of j_n in $T_{\rm EXC}$ are restricted to open-shell values, unless core-excited configurations occur in $|J_iT_i\rangle$.

These rules, and our other remarks, are easily established from the angular-momentum expansions for $\mathfrak{U}_{J_eT_e}$, reduced matrix elements, etc. The methods for expanding these quantities are given in detail in a number of places,[12] and their derivation here is unnecessary. Detailed expressions for these expansions are available from the author.

C. Specialization to Closed-Shell Targets

To carry out calculations using the results obtained so far requires that the configurations to be considered, as well as the target nucleus, be specified. It would then be necessary to carry out the various angular-momentum sums of $T_{\rm EXC}$. In this work we limit ourselves to the idealized case of a doubly magic nucleus, so that the target consists entirely of closed-shell configurations. For this case, it can be shown that nearly all the angular-momentum sums may be determined analyt-

[12] See, for example, Talmi and de-Shalit, Ref. 10.

ically and that T_{EXC} reduces to a very simple form. Hence, T_{EXC} becomes relatively easy to evaluate, which is consonant with our aims of obtaining an estimate of the size of T_{EXC}, and not in fitting particular data.

We therefore assume that the target nucleus is described by the state $|J_iT_i\rangle=|\prod_{j_c} j_c^{4j_c+2}(00)\rangle$ and that the final state is sufficiently low lying that it is simply $|J_fT_f\rangle=|\prod_{j_c} j_c^{4j_c+2}(00)j_0(j_0\frac{1}{2})\rangle$. Clearly, the quantities B_n are unity since only one configuration occurs. A further obvious point is that only the closed shells can contribute to T_{EXC}.

In order to compute the values of $\mathfrak{U}_{J_cT_c}$ we need three generalized cfp's, corresponding to: (1) removal of a particle in state $|j_c\frac{1}{2}\rangle$ from $|J_fT_f\rangle$, (2) removal of a particle in state $|j_0\frac{1}{2}\rangle$ from parents of $|J_fT_f\rangle$, and (3) removal of a particle in state $|j_c\frac{1}{2}\rangle$ from $|J_iT_i\rangle$. Expressions for these coefficients may be determined from the formulas of the Appendix. Once this is done, the quantities $B_\lambda{}^m(J_1J_2)$ of Eq. (17) can be evaluated. A straightforward and lengthy calculation yields the extremely simple formula

$$B_\lambda{}^m(J_1J_2)=[4\pi\alpha^2(A+1)^{1/2}]^{-1}i^{-l_0}\delta_{J_2\frac{1}{2}}\delta_{\lambda l_0}\times\sum_{kl_c}(2l_c+1)C^2(l_cl_0k;000)\times\langle k_p{}^{(-)}|\,\varphi_{l_c}V_{l_0kl_c}Y_{l_0}{}^{m*}|\,k_d{}^{(+)}\rangle. \quad (18)$$

In this equation, l_0 is the orbital angular momentum of the open shell in the residual nucleus corresponding to $l_0=j_0\pm\frac{1}{2}$ and is also the value of the transferred orbital angular momentum in the standard matrix element, T_{DWBA}. The quantity A is the number of target nucleons.

We note several interesting aspects of Eq. (18). First, only the values $J_2=\frac{1}{2}$ and $\lambda=l_0$ are allowed, so that $B_\lambda{}^m$ and $B_\lambda{}^M(J_1J_2)$ are completely coherent. Second, $B_\lambda{}^M(J_1J_2)$ is independent of the exchange nature of the two-body force, a result that follows since we are considering the interaction with a spherical, closed-shell nucleus, and it is known that in such a case the interaction is equivalent to that with a spherical well.[10] Finally, we see that all the closed shells (there is an implied summation on the principal quantum number in φ_{l_c}) contribute coherently so that there is constructive interference. That is, we have a cooperative effect among all A nucleons: this "collective" type of behavior could cause T_{EXC} to be large. No such simple expression arises, for example, when the (d,p) or (d,n) reaction is on a single-hole nucleus leading to the ground state of a doubly magic residual nucleus, despite the fact that the final state consists only of closed shells.

The corresponding expression for $B_\lambda{}^m$ is found to be[13]

$$B_\lambda{}^m=[\alpha^2(A+1)^{1/2}]^{-1}i^{-l_0}V(r_{np}=0)\delta_{\lambda l_0}\times\langle k_p{}^{(-)}|\,\varphi_{l_0}Y_{l_0}{}^{m*}|\,k_d{}^{(+)}\rangle. \quad (19)$$

[13] This expression for $B_\lambda{}^m$ takes into account the effect of the exchange operators occurring in Eq. (14) that are also present in V_{np}.

If we write the two-body force as $V(r_{ij})=V_0f(r_{ij})$, and also the multipole coefficient $v_k(r_i,r_j)$ as $V_0f_k(r_i,r_j)$, then Eqs. (18) and (19) are seen to differ only in the matrix elements $\mathfrak{M}_{\mathrm{DWBA}}$ and $\mathfrak{M}_{\mathrm{EXC}}$:

$$\mathfrak{M}_{\mathrm{DWBA}}=f(r_{np}=0)\langle k_p{}^{(-)}|\,\varphi_{l_0}Y_{l_0}{}^{m*}|\,k_d{}^{(+)}\rangle, \quad (20a)$$

$$\mathfrak{M}_{\mathrm{EXC}}=(4\pi)^{-1}\sum_{l_ck}(2l_c+1)C^2(l_cl_0k;000)\times\langle k_p{}^{(-)}|\,\varphi_{l_c}f_{l_0kl_c}Y_{l_0}{}^{m*}|\,k_d{}^{(+)}\rangle. \quad (20b)$$

It should be recalled that there is an implicit sum on the principal quantum number for each φ_{l_c} in Eq. (20b).

Specific forms for the φ_l and $f(r_{ij})$ were chosen in the present work. We used oscillator wave functions for the φ_l, with oscillator parameter b:

$$\varphi_l(r)=R_l(r)e^{-\frac{1}{2}(r/b)^2},$$

where R_l is a polynomial of degree l. For $f(r_{ij})$ we chose a Gaussian dependence:

$$f(r)=e^{-(r/r_0)^2},$$

so that $f(r=0)=1$. In all calculations we set $b=r_0$. Retaining different values of r_0 and b would conceivably alter the value of T_{EXC} by 15% or 20%, but we believe this to be ignorable since we are interested only in an order of magnitude estimate of T_{EXC}, which is all we can expect our calculations to give.[14]

With these assumptions, the $f_{l_0kl_c}$ of Eq. (20b) may be evaluated, if the closed-shell configurations are given. We have chosen as a target an idealized Ca^{40} nucleus, whose configurations are assumed to consist of all closed shells up through and including $d_{3/2}$. The residual nucleus was chosen to be $Ca^{41}=Ca^{40}+f_{7/2}$, where the value of j_0 added to the target nucleus is the extra open-shell configuration present in the final state.

A value for V_0 was determined by requiring $V_0\alpha^{-2}$ to give the same strength amplitude for T_{DWBA} as in the normal zero-range approximation. That is, we set $V_0\alpha^{-2}=(-\hbar^2/M)$. Then $V_0\approx-2$ MeV. This very small value of V_0 actually is an indication that the point-deuteron approximation is a poor means for estimating the strength of the amplitude: the deuteron wave function is simply too diffuse to be approximated by a delta function.

If we regard as a more reasonable value for $-V_0$ a number at least an order of magnitude larger than 2 MeV, then this implies that $\alpha^{-1}\lesssim 1.35$ F, which *is* small enough that the delta-function approximation is not too bad. Hence, the low value of V_0 may be regarded as a renormalization of α. Note that the renormalization is fully equivalent to including on the right-hand side of (C) a factor ξ, which can also be used to compensate for the inherent over-estimation associated with the

[14] All shells in the same nucleus were thus chosen to have the same value of b (or r_0). This should have a relatively small effect, since the difference in values of b for the $1p_{3/2}{}^-$ and the $1f_{7/2}{}^-$ shells, for example, is only about 10%.

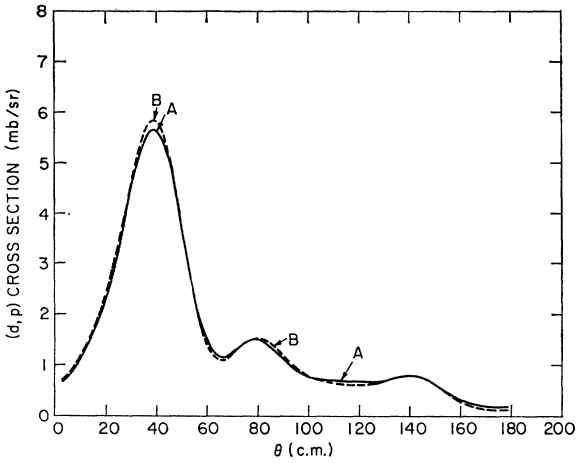

FIG. 1. Angular distributions at $E_d=11$ MeV: Curve (A) with target excitation; curve (B) with $T_{\mathrm{EXC}}=0$.

point-deuteron approximation. Had we done so, and chosen a reasonable value for V_0, say -50 MeV, then we would have found that the value $\xi=0.04$ was required to obtain the proper magnitude for T_{DWBA} as calculated in the zero-range approximation and noted above. Thus, the low value of $V_0=-2$ MeV (which, it should be recalled is common to *both* T_{DWBA} and T_{EXC}) is only to be regarded as a device that guarantees cross sections of the proper order of magnitude. The important point is that the ratio $T_{\mathrm{EXC}}/T_{\mathrm{DWBA}}$ is independent of V_0 (and of any extra parameter such as ξ, introduced above). It is this latter fact on which we have based the reliability of our estimates of the ratio $T_{\mathrm{EXC}}/T_{\mathrm{DWBA}}$.

III. CALCULATIONS

In order to calculate T_{DWBA} and T_{EXC}, it is necessary to specify r_0, the deuteron energy E_d, and the values of the optical-model parameters such as well depths, radial shapes, etc. Since our development of the amplitudes involves a number of approximations, it was decided to vary all of the above quantities, thus performing a computer experiment to determine the dependence of the amplitudes on r_0, E_d, etc. The numerical work was done on the IBM 7094 at Brookhaven National Laboratory using a code developed by W. R. Gibbs and modified by E. H. Auerbach to include both a fast search program and a means for computing T_{EXC}.

The reaction $Ca^{40}(d,p)Ca^{41}$ leading to the ground and excited states of Ca^{41} has been extensively studied, the most recent work being that of the Oak Ridge–Argonne collaboration.[15] Angular distributions for E_d taking on the values 7(1)12 MeV were measured for the ground-state and three excited-state transitions. An extensive program of fitting the data using different optical potentials was undertaken. Reasonable agreement with

[15] L. L. Lee, Jr., J. P. Schiffer, B. Zeidman, R. H. Bassel, R. M. Drisko, and G. R. Satchler, Phys. Rev. **136**, B971 (1964).

TABLE I. Comparison of optical-potential parameters used in the present work and in the Oak Ridge–Argonne Collaboration (Ref. 15).

	Present work	Oak Ridge–Argonne
V_d (MeV)	−105.0	−108.6
W_d (MeV)	−5.95	−7.77
R_d (F)	5.14	3.63,[a] 6.30[b]
a_d (F)	0.654	0.773,[a] 0.314[b]
V_p (MeV)	−50.0	−55.0
W_p (MeV)	−4.37	−11.0
R_p (F)	4.30	4.1,[a] 4.27[b]
a_p (F)	0.50	0.65,[a] 0.47[b]

[a] This value refers to the real part of the optical potential.
[b] This value refers to the imaginary part of the potential well.

the data was obtained for those potentials which also fit elastic-scattering data [particularly the (d,d) elastic scattering], and it was concluded that spectroscopic factors could be determined with an accuracy of 20% or better.

The code of Gibbs used in our numerical work employs the standard Woods-Saxon form factor for the radial shape of the optical potential; thus, the imaginary part is "volume absorption," with the same size parameters as the real part. The Oak Ridge–Argonne collaboration[15] also studied the case of volume absorption, and we decided first to see how well the $E_d=10$-MeV data could be fitted using our calculational method. That is, we regarded the results of Lee *et al.*[15] as a norm against which our results could be measured. Since our model of Ca^{40} is unrealistic,[16] and since our aim is to give an estimate of the size of T_{EXC}, rather than fit data, we do not show the results of our attempted fit to the experimental angular distribution. We simply remark here that the agreement was sufficiently encouraging, and the values of the optical potential parameters were close

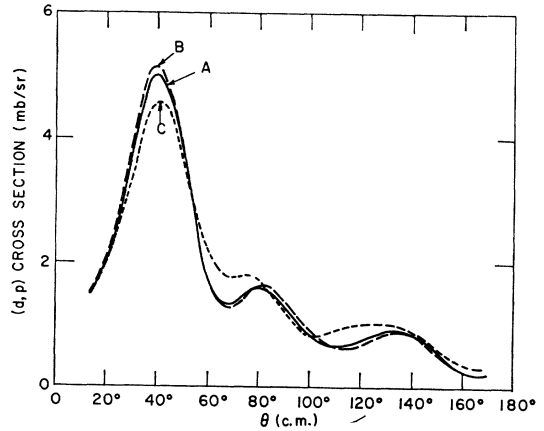

FIG. 2. Angular distributions at 10 MeV: Curve (A) with target excitation; curve (B) with $T_{\mathrm{EXC}}=0$; curve (C) with T_{EXC} five times as great as in curve (A).

[16] Recent experimental evidence for the nonclosed-shell nature of Ca^{40} ground state is given by R. Bock, H. H. Duhm, and R. Stock, Phys. Letters **18**, 61 (1965).

enough in value to the set VZ of Ref. 15, to warrant carrying out the remainder of our exploratory calculations. A comparison of the parameters of our calculation with those of set VZ (these are well parameters for the deuteron) and the set of proton parameters of Ref. 15 is given in Table I. Surface absorption was used in Ref. 15 for the proton optical potential, but this should not give significantly different fits to angular distributions, although better fits seem to be obtained using surface absorption or surface plus volume absorption.[17] The value $r_0=2.06$ F was used in conjunction with the optical-model parameters of Table I.

The second stage of the calculations was the determination of the energy dependence of the angular distributions calculated using the above mentioned set of parameters. We varied E_d in the range 3 MeV$\leq E_d \leq$12 MeV and in addition, we computed T_{DW}, and thus $d\sigma/d\Omega$, for T_{EXC} both zero and nonzero. The results of these calculations are shown in Figs. 1–6, with curves A based on $T_{\mathrm{DW}}=T_{\mathrm{DWBA}}+T_{\mathrm{EXC}}$ and curves B based on $T_{\mathrm{DW}}=T_{\mathrm{DWBA}}$ only. It is evident from these curves that inclusion of T_{EXC} decreases the over-all angular distribution due to T_{DWBA} alone by at most 5% and only 3% in the region of the stripping peak for all energies studied. An interesting feature of using oscillator wave functions is that the peak cross section occurs at 40° rather than 35° as observed experimentally at $E_d \geq 10$ MeV. Furthermore, the shift of the peak to larger angles as E_d decreases is much too pronounced in the theoretical calculations. However, use of a more realistic wave function in the amplitude T_{DWBA} alone corrected this behavior. Since both T_{DWBA} and T_{EXC} employ oscillator wave functions, we do not believe that this use strongly affects the value of the ratio $|T_{\mathrm{EXC}}/T_{\mathrm{DWBA}}|$.

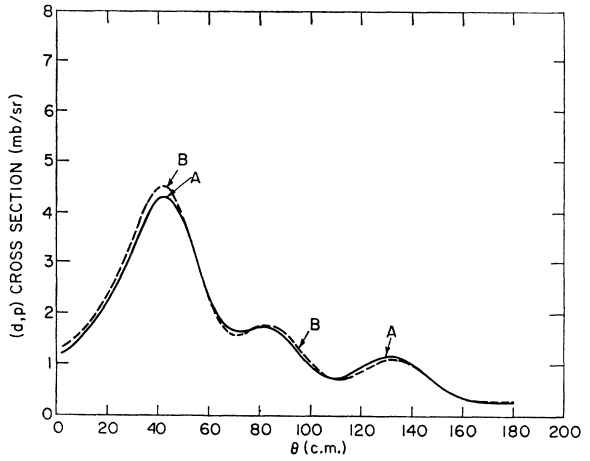

FIG. 3. Angular distributions at 9 MeV: Curve (A) with target excitation; curve (B) with $T_{\mathrm{EXC}}=0$.

[17] See comments of F. Perey, Phys. Rev. **131**, 745 (1963) and similar ones for the case of $Ca^{40}(d,d)Ca^{40}$ by R. H. Bassel, R. M. Drisko, G. R. Satchler, L. L. Lee, Jr., J. P. Schiffer, and B. Zeidman, Phys. Rev. **136**, B960 (1964).

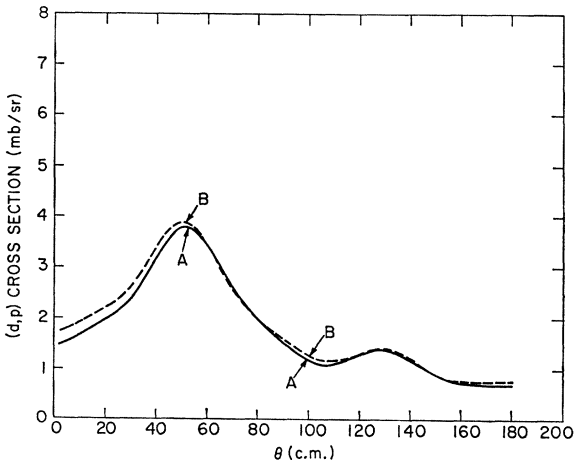

FIG. 4. Angular distributions at 7 MeV: Curve (A) with target excitation; curve (B) with $T_{\mathrm{EXC}}=0$.

For the $E_d=10$-MeV case, we also have included a calculation in which the magnitude of T_{EXC} was arbitrarily increased by a factor of 5, shown as curve C in Fig. 2. It will be seen that the shape of the angular distribution is not significantly altered from curves A and B, while the peak magnitude is decreased by 9% compared to curve B. Thus, even if we have underestimated T_{EXC} by 500%, the corrected amplitude would not produce substantially different results than those obtained from T_{DWBA} alone.

The general trends of curves A and B in Figs. 1–6 indicate that $\mathfrak{M}_{\mathrm{EXC}} \lesssim -0.02\mathfrak{M}_{\mathrm{DWBA}}$.[18] To help understand the small value of T_{EXC}, we have plotted in Fig. 7 the stripping "form factors" of Eqs. (20a) and (20b). For $\mathfrak{M}_{\mathrm{DWBA}}$ this form factor is simply φ_{l_0}, the single-particle radial wave function, plotted as curve A in Fig. 7. For $\mathfrak{M}_{\mathrm{EXC}}$, the form factor is given by $(4\pi)^{-1}\sum_{l_c k}(2l_c+1)C^2(l_c l_0 k;00)^2\varphi_{l_c} f_{l_0 k l_c}$, and is plotted as curve B in Fig. 7.

If we interpret the (d,p) reaction as a surface reaction, and so use the damping of the $|k_p^{(-)}\rangle$ and $|k_d^{(+)}\rangle$ in the interior of the nucleus plus the rapid fall off of the form factors with r, then we have a simple explanation of the small size of T_{EXC}: the distorted waves cannot reach that part of the nucleus to sample the form factor of $\mathfrak{M}_{\mathrm{EXC}}$ where it is large. The consequent small overlap in $\mathfrak{M}_{\mathrm{EXC}}$ thus produces a small amplitude T_{EXC}.

The above explanation is, however, incorrect. As discussed by Austern[19] and McCarthy,[20] the apparent surface nature of direct reactions is, in fact, due to complex interference effects that only permit certain partial waves to make large contributions to $\mathfrak{M}_{\mathrm{DWBA}}$. Since the structure of $\mathfrak{M}_{\mathrm{EXC}}$ is quite similar to that of $\mathfrak{M}_{\mathrm{DWBA}}$, we can expect interference effects similar to those of $\mathfrak{M}_{\mathrm{DWBA}}$ also to occur in $\mathfrak{M}_{\mathrm{EXC}}$. The behavior

[18] We note that $\mathfrak{M}_{\mathrm{DWBA}}$ and $\mathfrak{M}_{\mathrm{EXC}}$ have the same phase factor, viz., $e^{2i\pi}=+1$.

[19] N. Austern, Ann. Phys. (N. Y.) **15**, 299 (1961).

[20] I. E. McCarthy, Phys. Rev. **128**, 1237 (1962).

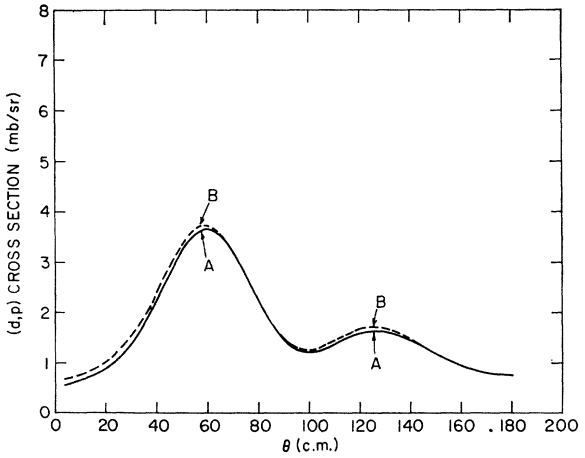

FIG. 5. Angular distributions at 5 MeV: Curve (A) with target excitation; curve (B) with $T_{EXC}=0$.

of $\mathfrak{M}_{DW}=\mathfrak{M}_{DWBA}+\mathfrak{M}_{EXC}$ may thus reflect the interplay of these two sets of coherently interfering partial waves. Such an interplay does occur, as indicated first by the size of T_{EXC} as determined by specific calculation, and second, by the fact that for certain choices of r_0 and the optical-model parameters, $\mathfrak{M}_{DW}=\mathfrak{M}_{DWBA}+\mathfrak{M}_{EXC}>\mathfrak{M}_{DWBA}$ implying that $\mathfrak{M}_{EXC}$ has the *same* sign as $\mathfrak{M}_{DWBA}$, in contrast to the results of Figs. 1–6.

The above remark about the size of T_{EXC} is easily verified from Fig. 8, where we plot $d\sigma/d\Omega$ due to T_{EXC} alone for $E_d=10$ MeV, $r_0=2.06$ F and the optical-model parameters of Table I. Comparison of the peak value of Fig. 8 with that of curve B of Fig. 2 gives $T_{EXC}/T_{DWBA}\approx 0.06$, a factor of *three* larger than implied by Figs. 1–6. The fact that inclusion of T_{EXC} fails to change by 12% the angular distribution arising from T_{DWBA} alone is thus a strong piece of evidence that $\mathfrak{M}_{EXC}$ introduces additional interference effects into T_{DW}, rather than simply adding linearly, as would a constant. That the

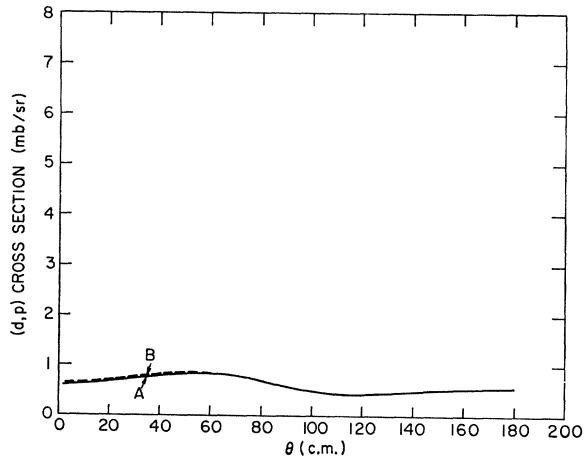

FIG. 6. Angular distributions at 3 MeV: Curve (A) with target excitations; curve (B) with $T_{EXC}=0$.

TABLE II. Range of values considered in variation of the optical-model parameters. Well depths are given in MeV, shape parameters in F.

V_d	V_p	W_d	W_p	R_d	R_p	a_d	a_p
−120	−60	−10	−8, −10	5.50	5.00	0.70	0.55
−90	−40	−4	−3	4.50	4.00	0.60	0.45

sign of $\mathfrak{M}_{EXC}/\mathfrak{M}_{DWBA}$ varies is borne out by the calculations discussed below.

The shape of the curve of Fig. 8 is also of interest, but we postpone discussion of it until we consider the shapes of the curves obtained by varying the parameters of our model.

The third and final stage of our calculational program was a study of the effect on T_{DW} and T_{EXC} of changing r_0 and the optical-model parameters by roughly 15% or 20% of the values used to obtain Figs. 1–8. Calculations were carried out for $E_d=5$ MeV and $E_d=10$ MeV, with r_0 taking on the values 1.95, 2.06, and 2.20 F. The optical-potential parameters used in this part of the calculation are given in Table II. The method of parameter variation was as follows: First, all proton and deuteron parameters were fixed at the values of Table I, while E_d and r_0 varied as stated above. Second, both proton- and deuteron-shape parameters were fixed ad the values of Table I and the well depths were allowed to assume all values in Table II, with concomitant changes in r_0 and E_d. Finally, the proton and deuteron well depths were fixed as in Table I, r_0 was kept equal

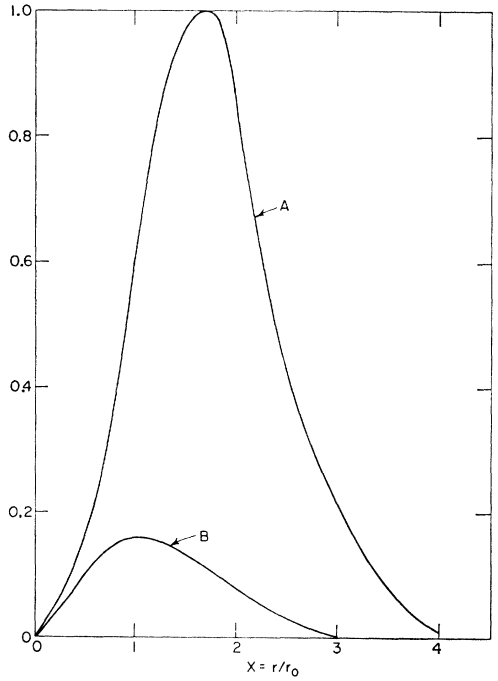

FIG. 7. Radial shape for form factors (see text): Curve (A) form factor for T_{DWBA}; curve (B) form factor for T_{EXC}.

to 2.06 F, and the shape parameters were varied as in Table II for $E_d=5$ and 10 MeV.

Rather than display a large number of curves illustrating the results, we list the general trends arising from our calculations. The following notation is used: σ_{DW} is the angular distribution arising from $T_{\mathrm{DW}}=T_{\mathrm{DWBA}}+T_{\mathrm{EXC}}$; σ_{DWBA} is the angular distribution arising from T_{DWBA} alone; σ_{EXC} is the angular distribution arising from T_{EXC} alone.

1. As r_0 increases, both σ_{DW} and σ_{DWBA} increase in magnitude, and σ_{EXC} decreases in magnitude.

2. All cross sections increase in magnitude as E_d increases.

3. Increasing W_p causes all cross sections to decrease.

4. As W_d increases, σ_{DW} and σ_{DWBA} increase for $E_d=10$ MeV and decrease for $E_d=5$ MeV. However, in all instances but the exceptional cases noted below, σ_{EXC} decreases with increasing W_d for both values of E_d.

5. There are no systematic variations in any of the angular distributions as either V_d or V_p is changed.

6. Both σ_{DW} and σ_{DWBA} decrease as R_d is increased, while σ_{EXC} correspondingly increases.

7. Changing a_d leaves both σ_{DW} and σ_{DWBA} relatively unchanged, while σ_{EXC} increases with increasing a_d.

8. All cross sections are relatively independent of changes in R_p and a_p.

9. For fixed values of E_d and V_p or V_d, the position of peaks in angular distributions remains the same to within approximately $\pm 6°$ for changes in r_0 or W.

10. Variations in E_d, V_d, or V_p lead to no systematic variations of the position of peak cross sections.

11. σ_{EXC} generally exhibits one or more very broad peaks. By proper choice of the optical-potential parameters and r_0 those can be made to have a first maximum nearly anywhere in the range 0°–80°.

12. Finally, except as noted below, the magnitude of σ_{DW} differs by no more than 6% (over the whole angular range) when compared with σ_{DWBA}; $|T_{\mathrm{EXC}}/T_{\mathrm{DWBA}}|\leq 0.06$; and $\mathfrak{M}_{\mathrm{EXC}}/\mathfrak{M}_{\mathrm{DWBA}}$ is both positive and negative.

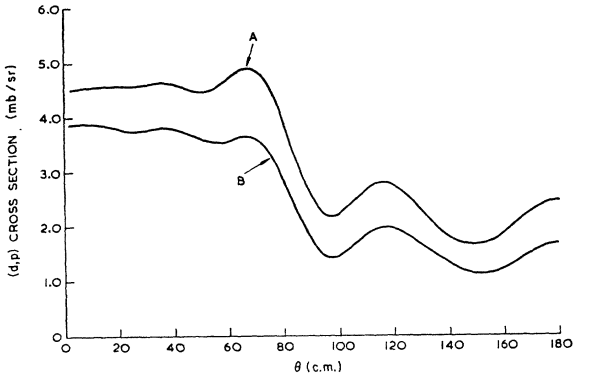

FIG. 9. Angular distributions at 10 MeV, $r_0=1.95$ F: Curve (A) with target excitation; curve (B) with $T_{\mathrm{EXC}}=0$.

The general result, expressed above in item 12, that T_{EXC} makes a small contribution to σ_{DW} is encouraging, since it implies that previous analyses based on T_{DWBA} alone have not omitted an important term in the amplitude. However, the existence of certain exceptions does not make the preceding statement an inevitable conclusion. Instead, these exceptions would seem to make more accurate calculations a necessity, especially in view of the possibility of explaining certain forbidden stripping reactions and low cross-section stripping reactions in terms of a target-excitation model, a point we discuss in the next section. The exceptions that have been referred to above are cases in which $|T_{\mathrm{EXC}}/T_{\mathrm{DWBA}}|\geq 0.06$ and the change in σ_{DW} resulting from the inclusion of T_{EXC} ranges from 10% to nearly 40%. The majority of these instances are for $V_d=-90$ MeV and $r_0=1.95$ F and occur for both the large and small values of W_p or W_d listed in Table II, as well as for either value of V_p or E_d. No such large effects are found for

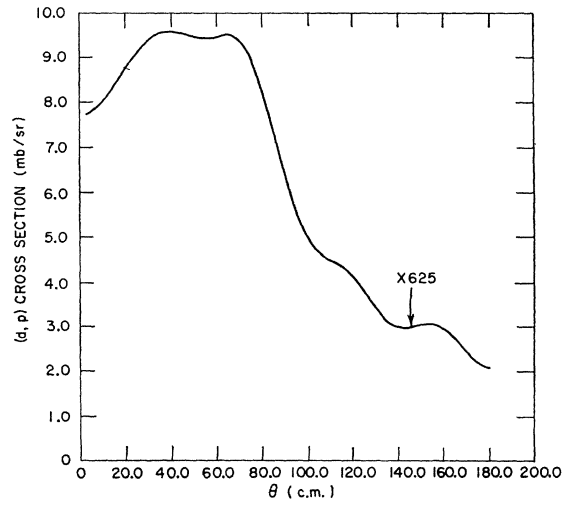

FIG. 8. Angular distribution due to T_{EXC} alone, $E_d=10$ MeV.

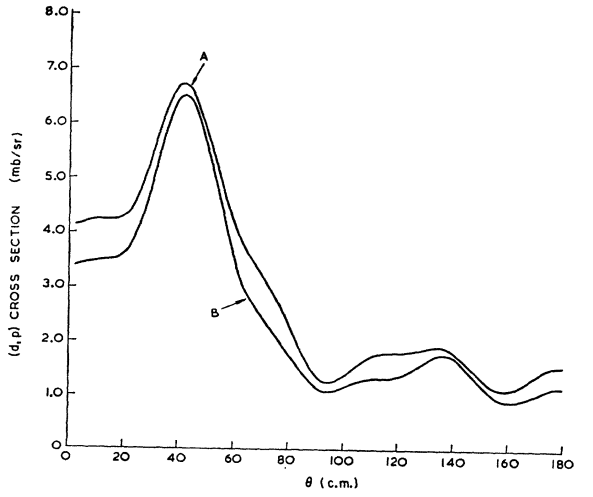

FIG. 10. Angular distributions at 10 MeV, $r_0=2.06$ F: Curve (A) with target excitation; curve (B) with $T_{\mathrm{EXC}}=0$.

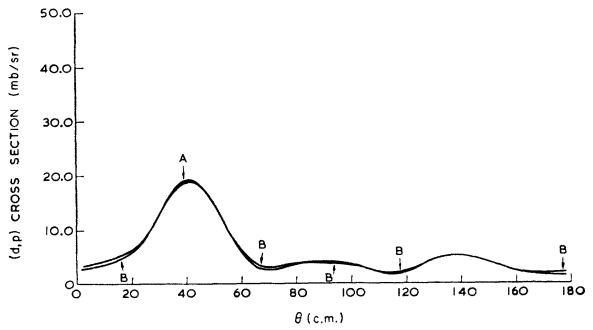

FIG. 11. Angular distributions at 10 MeV, $r_0=2.20$ F: Curve (A) with $T_{\mathrm{EXC}}=0$; curve (B) with target excitation.

$r_0=2.20$ F, and only a few occur for $r_0=2.06$ F, including the case $R_d=5.5$ and both values of a_d and E_d[21] (recall that for this variation, V_d, V_p, W_d, R_p, and a_p are as given in Table I), for which the change in σ_{DW} is slightly more than 10%. However, the total number of cases in this category was only 15 of the more than 160 cases considered.

The angular distributions for these exceptional cases do not show a consistent pattern: wide variation in the position and widths of the diffraction peaks occur. It is interesting to note that the shape of σ_{EXC} remains much the same as r_0 is varied at fixed values of energy and well parameters. However the shapes of σ_{DW} and σ_{DWBA}, though similar, vary with r_0 and do not resemble σ_{EXC}. This is especially interesting since σ_{DW} and σ_{DWBA} can differ by 25% or more in magnitude.

These remarks are illustrated in Figs. 9–12. The energy here was fixed at $E_d=10$ MeV and the well depths used to calculate the distorted waves were $V_d=-90$ MeV, $W_d=-4$ MeV, $V_p=-60$ MeV, and $W_p=-8$ MeV with the remaining well parameters held at the values of Table I. Figures 9, 10, and 11 show both σ_{DW} and σ_{DWBA} for $r_0=1.95$, 2.06, and 2.20 F, respectively, while Fig. 12 shows σ_{EXC} for the various values of r_0. It is evident that σ_{DW} and σ_{DWBA} are quite similar for each value of r_0 while σ_{EXC} is noticeably different. Also, σ_{EXC} maintains the same general shape for different r_0, even though σ_{DW} and σ_{DWBA} are changing with r_0. The interference effects noted above are apparent in these curves, since in Figs. 9 and 10, $\sigma_{\mathrm{DW}}>\sigma_{\mathrm{DWBA}}$, while in Fig. 11, some portions of σ_{DW} are less than the corresponding segments of σ_{DWBA}. As these are the exceptional cases, all three cross sections are seen to increase with increasing r_0, although the effect of T_{EXC} is greatest for $r_0=1.95$ F and then becomes significantly smaller as noted in preceding paragraphs.

For other values of the well parameters, the shapes of σ_{DW} and σ_{DWBA} can differ from those of Figs. 9–11. Included are angular distributions with a sharp peak at 0° and those with four or five peaks spaced over the entire angular range and of nearly equal magnitude. On the other hand, the shapes of σ_{EXC} do not show such wide variations. This is seen on comparison of Figs. 8 and 12.

[21] Similar effects do not occur for variations in R_p and a_p.

We have found only a few cases of σ_{EXC} exhibiting the truly sharp diffraction peak characteristic of the usual stripping process. The general shape of σ_{EXC} is that given in item 11 above. We discuss this behavior in the next section.

IV. DISCUSSION AND CONCLUSIONS

The general conclusion implied by our calculations is that T_{EXC} is small enough to be ignored. However, this conclusion must be tentative, and to a large extent may be weakened, because of both the crudity of our models and the presence of the exceptions noted in the preceding section.

Let us discuss the exceptions first. We note that they are obtained when values of the complex well parameters are used that differ from those associated with elastic scattering. Now, at the present stage of understanding of both the optical model of elastic scattering and the distorted-wave model of direct reactions, we have no valid theoretical reasons for believing that the elastic well parameters should be used in (d,p) analyses. Thus, even though well parameters other than those for elastic scattering may produce a σ_{DWBA} not in agreement with experiment, this is not necessarily an argument against their use, since the distorted-wave model in its standard form still remains to be validated. Future developments may point to use of such well parameters, or may suggest other approximations.[22] We see that the finding of exceptional cases is closely connected with the validity of the distorted-wave model. This is not unexpected in a situation where a multiparameter model is used to fit data and in which small deviations from a set of parameters can drastically change the results. A similar dependence on the well parameters has also been found by Kozlowsky and de-Shalit in their study of the (He^3,d) reaction proceeding by a pure core-excitation process.[23] These authors have found that the size of T_{EXC}, as calculated in their model, is strongly dependent on the radius of the imaginary part of the deuteron optical potential as compared to the radius of the real part of the well. Although in the present work and in that of Kozlowsky and de-Shalit different nuclear models are used, both find a strong dependence of T_{EXC} on the well parameters. It is clear that further investigations are necessary before this particular dependence can be understood.

We now consider the nuclear models we have used to help evaluate T_{EXC}. There are three aspects involved: first, the use of the point-deuteron assumption; second, the assumption of a closed-shell target; and third, the use of oscillator wave functions to evaluate the factors $V_{lkl'}$, and the matrix element $\mathfrak{M}_{\mathrm{EXC}}$.[24]

[22] B. Buck and J. R. Rook, Nucl. Phys. **67**, 504 (1965) and to be published.

[23] A. de-Shalit, Brookhaven National Laboratory Report No. BNL 948, 1965 (unpublished), p. 552; and to be published.

[24] As noted in the preceding section, we do not believe the assumed equality of r_0 and b to be an important factor and we consequently ignore it.

The point-deuteron approximation has already been discussed and we believe that its main features are understood and its shortcomings accounted for. Verification of this statement can only be obtained by a specific calculation, but we shall assume that this particular approximation does not strongly affect our results.

Use of the idealized closed-shell target nucleus allowed us to obtain a very simple expression for T_{EXC}, although such an idealized nucleus has no natural counterpart. Since the final nucleus is closed shell plus one, we might imagine that this case is, theoretically, the one most likely to give a minimum value for $|\mathfrak{M}_{\mathrm{EXC}}/\mathfrak{M}_{\mathrm{DWBA}}|$, since $\mathfrak{M}_{\mathrm{DWBA}}$ is a maximum (spectroscopic factor of unity). While it is to be expected that the use of model wave functions containing several open-shell configurations will reduce the size of $\mathfrak{M}_{\mathrm{DWBA}}$, we must anticipate that in this more general case $\mathfrak{M}_{\mathrm{EXC}}$ will also be reduced in magnitude. The reason for this is to be found in the general formula for T_{EXC}, which contains many angular-momentum sums involving 3-j, 6-j, and 9-j coefficients as well as additional generalized cfp's. These latter do not occur in T_{DWBA}. The combination of the generalized cfp's and recoupling coefficients will tend to reduce the size of $\mathfrak{M}_{\mathrm{EXC}}$ thus obtained as compared with $\mathfrak{M}_{\mathrm{EXC}}$ given in Eq. (20b). (Conservative estimates of the reduction factor lie in the range of 1/3 to 1/50.) Hence, we may assume that the use of an idealized doubly magic target to evaluate $\mathfrak{M}_{\mathrm{EXC}}$ gives results that are typical even for a much more realistic model.

The use of oscillator wave functions for the single-particle states is, we believe, the crudest of the several assumptions made in evaluating $\mathfrak{M}_{\mathrm{EXC}}$. This is already evident in the dependence of our results on the parameter r_0 and also in our lack of an external criterion for choosing any one particular value. However, another defect is the reduction in size of $\mathfrak{M}_{\mathrm{EXC}}$ due to the short range of the oscillator functions. This occurs through the presence of the two oscillator functions in $V_{lkl'}$. Because of their short range, these functions will cut down the size of $V_{lkl'}$ as compared with the result to be obtained by using wave functions with longer tails. An increase of only 15% in the contribution of each nuclear wave function that contributes to $V_{lkl'}$ will mean an increase of $V_{lkl'}$ over the values found herein by 30%. While this may not have strong effect on σ_{DW}, as indicated by curve C of Fig. 2, it would increase σ_{EXC}, a point we shall examine shortly. A further point along this line concerns the use of one value of b (viz., $b=r_0$) in all oscillator wave functions. Now the values of b used are too large ($b\approx 1.67$ F for 1p-shell nuclei), though we have ignored this. Use of more realistic wave functions not only would eliminate the bad choice of b, it conceivably could increase the size of $\mathfrak{M}_{\mathrm{EXC}}$ and thus of σ_{EXC}.

We have argued in the above that it is possible for

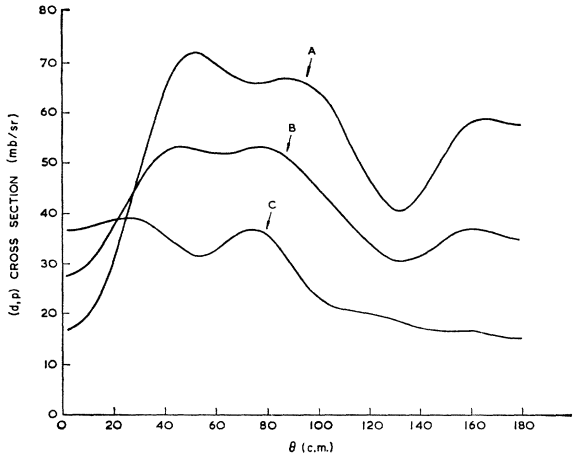

FIG. 12. Angular distributions at 10 MeV due to T_{EXC} alone: Curve (A) $r_0=2.20$ F; curve (B) $r_0=2.26$ F; curve (C) $r_0=1.95$ F.

$\mathfrak{M}_{\mathrm{EXC}}$ to assume values larger than implied by the majority of our numerical calculations. Some means for doing this are through the use of optical-potential well parameters not associated with elastic scattering; by the occurrence of strong configuration mixing in the nuclear states; or by use of more realistic wave functions. Although this may not alter the shapes of σ_{DWBA}, as indicated by our calculations, it is conceivable that the target-excitation process can then be used to account for certain stripping processes, hitherto unexplained. These are (d,p) and (d,n) angular distributions whose peak magnitudes are in the range of 1/20 to 1/100 of the peak magnitude of a cross section to a strongly excited state (theoretical spectroscopic factor near to unity); and (d,p) or (d,n) reactions for which T_{DWBA} is zero because of selection rules.

Numerous examples of the former type of angular distribution have been reported in the literature, with the shapes of the angular distributions seen to have a great variation, occasionally having a partial resemblance to particular l-value stripping patterns. The magnitudes of these cross sections often are between 0.01 and 0.05 of those to the ground state or a strongly excited state. These values could be obtained by σ_{EXC} using one or more of the means mentioned above.

Instances of the second type of angular distribution, observed when T_{DWBA} vanishes, are also known. Perhaps the most famous of these "forbidden" stripping reactions is $B^{10}(d,p)B_{2.14}$.[11]* Despite the many attempts[25]

[25] A. P. French, Phys. Rev. **109**, 1272 (1958); J. E. Bowcock, *ibid.* **112**, 923 (1958); B. Neudachin, Zh. Eksperim. i Teor. Fiz. **35**, 1165 (1959); B. G. Neudachin *et al.*, *ibid.* **37**, 548 (1959) [English transls.: Soviet Phys.—JETP **8**, 815 (1959); **10**, 387 (1960)]; G. E. Owen and W. Reichelt, Phys. Rev. **121**, 547 (1961); N. Menyhard and S. Zimanyi, Nucl. Phys. **29**, 687 (1962); M. Tanifuji, *ibid.* **40**, 357 (1963). In addition to none of these authors being able to explain the energy dependence of the cross sections, they all employ the Born approximation (in various types of matrix elements). In addition, some obtain nonzero results for matrix elements that can be shown to vanish.

to explain the occurrence of this reaction, none have succeeded in accounting for the main features of the reaction, viz., the appearance of an $l=1$ type peak at 30°, a secondary peak at 80°, and especially the over-all energy dependence of the reaction. We suggest here that the target-excitation process can be used to explain the occurrence of these forbidden reactions.

The above suggestions are, at the present stage of understanding, only speculations. Whether or not for example, σ_{EXC} can be made to display the sharp peaks of the $B^{10}(d,p)B_{2.14}{}^{11*}$ reaction, can only be decided by a direct calculation using more realistic models. The evidence at the present time, both from our work and that of other investigators,[26] is not favorable. It is, therefore, of interest to seek methods other than those based solely on evaluation of angular distributions that would test the target-excitation hypothesis. One such method is the measurement of angular corrections.

Let us consider a (d,p) or (d,n) reaction leading to a nuclear state of spin J_f that decays by gamma-ray emission. The angular distribution $W(\theta,\phi)$ of gamma rays relative to the direction of the outgoing proton is of the form[27]

$$W(\theta,\phi)=\sum_{\lambda\mu} A_{\lambda\mu}C_{\lambda\mu}(\theta,\phi),$$

with

$$C_{\lambda\mu}(\theta,\phi)=[4\pi/(2\lambda+1)]^{1/2}Y_{\lambda}{}^{\mu}(\theta,\phi).$$

The aspect of $W(\theta,\phi)$ we wish to consider here is the maximum value of λ, denoted $\lambda_{\max}$. In general,

$$\tfrac{1}{2}\lambda_{\max}=\min(L,[J_f]),$$

where L is the multipolarity[28] of the gamma ray and $[J_f]$ is the largest integer contained in J_f. If T_{DWBA} is the only amplitude that contributes to the angular distribution, then an additional restriction on $\lambda_{\max}$ is $\frac{1}{2}\lambda_{\max}\leq[j_n]$, where j_n is the angular momentum of the captured nucleon. However, if T_{EXC} also contributes to the angular distribution, then the additional restriction on $\lambda_{\max}$ is not $\frac{1}{2}\lambda_{\max}\leq[j_n]$ but $\frac{1}{2}\lambda_{\max}\leq[J]$, where J itself is restricted by the triangle relation $\Delta(J_iJ_fJ)$ and also by other model-dependent relations. The new restriction, $\frac{1}{2}\lambda_{\max}\leq[J]$, is independent of the model used to evaluate T_{EXC}, and is derived directly from Eq. (8). For our shell-model calculation of T_{EXC}, the additional restrictions on J follow from the fact that $J=J_1$ of Eq. (17): we thus have $\Delta(j_0kJ)$ and $\Delta(j_ckJ)$, where k labels the multipolarity of the two-body force and j_0 and j_c are the open- and closed-shell angular momenta. These latter restrictions on $J(=J_1)$ come from the shell-model assumption alone and are not limited to the closed-shell target case. Other nuclear models will provide a different set of additional restrictions on J. Obviously, the coefficients $A_{\lambda\mu}$ will also depend on the model used to evaluate T_{EXC}, and can be calculated when the model is specified, but we do not consider them further here.

The possible application of angular-correlation measurements to the problem of identifying the presence of T_{EXC} is now evident, although favorable cases will be needed. That is, $[j_n]$ is usually limited to a specific value because of the nuclear model, whereas $[J]$ may be allowed to take on a larger value than does $[j_n]$. Hence, in favorable cases, the presence of T_{EXC} will lead to a larger value of $\lambda_{\max}$ than allowed by $[j_n]$, and thus an extra term (or terms) in $W(\theta,\phi)$ will arise, due *entirely* to T_{EXC} [in our model of direct (d,p) and (d,n) reactions].

Of course, experimental observation of terms in $W(\theta,\phi)$ forbidden on the assumption that $T_{\mathrm{DW}}=T_{\mathrm{DWBA}}$, is not necessarily an indication that T_{EXC} is making a non-negligible contribution. Other processes could be occurring that would give rise to the additional terms in $W(\theta,\phi)$. However, if the energy is sufficiently large, say $E_d\gtrsim 10$ MeV for light nuclei ($A\lesssim 60$) *and* if the experimental angular distribution displays the usual forward peaking and/or diffraction behavior associated with direct reactions, then we have good reason to expect that target excitation is playing a role in the reactions. To minimize the possible role of exchange amplitudes, the outgoing proton angle should be in the forward direction, thus assuring that the terms in T_{DW} we have considered are dominant. Under these circumstances, we have a necessary criterion for T_{EXC} to be present, but unfortunately, not a sufficient one. That is, T_{EXC} could be strong, but $[J_1]=[j_n]$, and no additional effects will be observed in $W(\theta,\phi)$. Despite this, we believe that gamma-ray measurements provide a simple means for identifying at least some cases where T_{EXC} is non-negligible; a model can then be invoked and T_{EXC} evaluated and compared to T_{DWBA}.

ACKNOWLEDGMENTS

The author wishes to thank W. R. Gibbs for supplying the distorted-wave code, and E. Auerbach and L. Bargiuk for modifying and testing the code. He also thanks G. R. Satchler and W. T. Pinkston for illuminating discussions on the role of the V_{pt} interaction and J. Weneser for a number of clarifying remarks. Finally, he thanks D. Amit for helpful correspondence concerning the generalized fractional-parentage coefficients.

[26] As yet unpublished numerical results indicating that T_{EXC} is small have been obtained by G. R. Satchler and S. K. Penney, D. Dillenburg, and R. Sorenson, and P. Iano, and N. Austern (private communication from N. Austern). See, also, S. K. Penney and G. R. Satchler, Nucl. Phys. **53**, 145 (1964); and D. Dillenburg and R. Sorenson, Bull. Am. Phys. Soc. **10**, 40 (1965). Spectroscopic factors, including the effect of target excitation have been calculated by W. Beres, Phys. Letters **16**, 65 (1965), using the model employed by Koslowsky and de-Shalit and Dillenburg and Sorenson.

[27] G. R. Satchler and W. Tobocman, Phys. Rev. **118**, 1566 (1961); R. Huby, M. Y. Refai, and G. R. Satchler, Nucl. Phys. **9**, 94 (1958).

[28] We assume, for simplicity, that only one multipole is involved.

APPENDIX

The formulas for the generalized cfp's are obtained in a straightforward manner using the recoupling techniques introduced by Racah.[29] Let $[|J_1T_1\rangle\otimes|J_2T_2\rangle]_{JT}$ represent the state $|JT\rangle$ obtained by vector coupling together the states $|J_1T_1\rangle$ and $|J_2T_2\rangle$ by means of Wigner coefficients. Then the full cfp expansion of the typical state as given by Eq. (10) is

$$
\begin{aligned}
&|\prod_{j_c} j_c^{4j_c+2}(00)j'^a(J_n'T_n'\alpha_n')j''^b(J_n''T_n''\alpha_n'');JT\rangle \\
&=\sum_{\substack{J_2T_2\alpha_2\\ J_eT_e\alpha_e}}\{([j'^{a-1}(J_2T_2\alpha_2)j''^b(J_n''T_n''\alpha_n'')](J_eT_e\alpha_e),j'[\![JT)[|j'^{a-1}(J_2T_2\alpha_2)j''^b(J_n''T_n''\alpha_n'');J_eT_e\rangle\otimes|j'^{\frac{1}{2}}\rangle]_{JT} \\
&\quad+([j'^a(J_n'T_n'\alpha_n')j''^{b-1}(J_2T_2\alpha_2)](J_eT_e\alpha_e),j''[\![JT)[|j'^a(J_n'T_n'\alpha_n')j''^{b-1}(J_2T_2\alpha_2);J_eT_e\rangle\otimes|j''^{\frac{1}{2}}\rangle]_{JT}\} \\
&\quad+\sum_{j_c}\sum_{J_eT_e\alpha_e}(\{[j'^a(J_n'T_n'\alpha_n')j''^b(J_n''T_n''\alpha_n'')](JT)j_c^{4j_c+1}(j_c\tfrac{1}{2})\}(J_eT_e\alpha_e),j_c[\![JT) \\
&\qquad\times[|\{j'^a(J_n'T_n'\alpha_n')j''^b(J_n''T_n''\alpha_n'')](JT)j_c^{4j_c+1}(j_c\tfrac{1}{2});J_eT_e\alpha_e\rangle\otimes|j_c\tfrac{1}{2}\rangle]_{JT}. \qquad \text{(A1)}
\end{aligned}
$$

Since removal of a nucleon in a particular state changes only the quantum numbers of the group from which the nucleon came, we have omitted all closed shells on the right-hand side of Eq. (A1), as they do not enter the calculation. It is clear that the group $j_c^{4j_c+2}(00)$ can be moved to the right of the open-shell nucleons without the introduction of a phase factor. We also note that the total number of nucleons N is given by $N=a+b+\sum_{j_c}(4j_c+2)$.

An alternative form for the cfp expansion is in terms of the single-configuration cfp's:

$$
\begin{aligned}
&|\prod_{j_c} j_c^{4j_c+2}(00)j'^a(J_n'T_n'\alpha_n')j''^b(J_n''T_n''\alpha_n'');JT\rangle \\
&=\sum_{J_2T_2\alpha_2}\left\{\left(\frac{a}{N}\right)^{1/2}(j'^{a-1}(J_2T_2\alpha_2),j'[\![j'^a(J_n'T_n'\alpha_n'))|[j'^{a-1}(J_2T_2\alpha_2)j']j''^b(J_n''T_n''\alpha_n'');JT\rangle\right. \\
&\quad\left.+\left(\frac{b}{N}\right)^{1/2}(j''^{b-1}(J_2T_2\alpha_2),j''[\![j''^b(J_n''T_n''\alpha_n''))|j'^a(J_n'T_n'\alpha_n')[j''^{b-1}(J_2T_2\alpha_2)j'']j''^b(J_n''T_n''\alpha_n'');JT\rangle\right\} \\
&\quad+\sum_{j_c}\left[\frac{4j_c+2}{N}\right]^{1/2}(j_c^{4j_c+1}(j_c\tfrac{1}{2}),j_c[\![j_c^{4j_c+2}(00)) \\
&\qquad\times|[j'^a(J_n'T_n'\alpha_n')j''^b(J_n''T_n''\alpha_n')](JT\alpha)[j_c^{4j_c+2}(j_c\tfrac{1}{2})j_c](00);JT\rangle. \qquad \text{(A2)}
\end{aligned}
$$

In each of the states on the right-hand side of Eq. (A2), the single nucleon state can be brought to the right and coupled to the resulting angular-momentum state of all the other nucleons by using the recoupling techniques.[29] Doing so, and comparing with Eq. (A1), we find the following results:

$$
\begin{aligned}
&([j'^{a-1}(J_2T_2\alpha_2)j''^b(J_n''T_n''\alpha_n'')]J_eT_e\alpha_e),j'[\![JT) \\
&\quad=(a/N)^{1/2}(j'^{a-1}(J_2T_2\alpha_2),j'[\![j'^a(J_n'T_n'\alpha_n'))[(2J_e+1)(2J_n'+1)(2T_e+1)(2T_n'+1)]^{1/2} \\
&\qquad\times W(J_n'J_n''j'J_e;JJ_2)W(T_n'T_n''\tfrac{1}{2}T_e;TT_2), \qquad \text{(A3)} \\
&([j'^a(J_n'T_n'\alpha_n')j''^{b-1}(J_2T_2\alpha_2)](J_eT_e\alpha_e),j''[\![JT) \\
&\quad=(b/N)^{1/2}(j''^{b-1}(J_2T_2\alpha_2),j''[\![j''^b(J_n''T_n''\alpha_n'')) \\
&\qquad\times[(2J_e+1)(2J_n''+1)(2T_e+1)(2T_n''+1)]^{1/2}W(J_n'J_2Jj'';J_eJ_n'')W(T_n'T_2T\tfrac{1}{2};T_eT_n''), \qquad \text{(A4)} \\
&(\{[j'^a(J_n'T_n'\alpha_n')j''^b(J_n''T_n''\alpha_n'')](JT\alpha)j_c^{4j_c+1}(j_c\tfrac{1}{2})\}(J_eT_e\alpha_e),j_c[\![JT) \\
&\qquad=-N^{-1/2}(-1)^{J_e-J-j_c+T_e-T-1/2}[(2J_e+1)(2T_e+1)/(2J+1)(2T+1)]^{1/2}. \qquad \text{(A5)}
\end{aligned}
$$

These cfp's are normalized to unity as long as we assume the single configuration cfp's to be so normalized. The minus sign in Eq. (A5) arises because the closed-shell cfp appearing in Eq. (A1) is equal to minus one.

In addition to the above results, we also need the cfp for removal of an originally open-shell nucleon when one of the closed-shell nucleons has been removed. The daughter state is, for example, given by the $|J_eT_e\rangle$ state in the

---

[29] G. Racah, Phys. Rev. **63**, 367 (1943).

last summation of Eq. (A1). The same methods are used to treat this state as in the preceding; we obtain

$$(\{[j'^{a-1}(J_3T_3\alpha_3)j''^{b}(J_n''T_n''\alpha_n'')](J_4T_4\alpha_4)j_c^{4j_c+1}(j_c\tfrac{1}{2})\}(J_5T_5\alpha_5),j'[\![J_eT_e\alpha_e)$$

$$=\left(\frac{a}{N-1}\right)^{1/2}(j'^{a-1}(J_3T_3\alpha_3),j'[\![j'^{a}(J_n'T_n'\alpha_n'))$$

$$\times[(2J_n'+1)(2T_n'+1)(2J+1)(2T+1)(2J_4+1)(2T_4+1)(2J_5+1)(2T_5+1)]^{1/2}$$

$$\times W(J_n'J_n''j'J_4;J_eJ_3)W(T_n'T_n''\tfrac{1}{2}T_4;T_eT_3)W(Jj_cj'J_5;J_eJ_4)W(T\tfrac{1}{2}\tfrac{1}{2}T_5;T_eT_4) \quad \text{(A6)}$$

and

$$(\{[j'^{a}(J_n'T_n'\alpha_n')j''^{b-1}(J_3T_3\alpha_3)](J_4T_4\alpha_4)j_c^{4j_c+1}(j_c\tfrac{1}{2})\}(J_5T_5\alpha_5),j''[\![J_eT_e\alpha_e)$$

$$=\left(\frac{b}{N-1}\right)^{1/2}(j''^{b-1}(J_3T_3\alpha_3),j''[\![j''^{b}(J_n''T_n''\alpha_n''))$$

$$\times[(2J_n''+1)(2T_n''+1)(2J+1)(2T+1)(2J_4+1)(2T_4+1)(2J_5+1)(2T_5+1)]^{1/2}$$

$$\times W(J_n'J_3Jj'';J_4J_n'')W(T_n'T_3T\tfrac{1}{2};T_4T_n'')W(Jj_cj''J_5;J_eJ_4)W(T\tfrac{1}{2}\tfrac{1}{2}T_5;T_eT_4). \quad \text{(A7)}$$

PHYSICAL REVIEW VOLUME 147, NUMBER 3 22 JULY 1966

Direct Numerical Solution of the Three-Body Problem

S. ROSATI
Istituto di Fisica dell'Università, Pisa, Italy
and
Istituto Nazionale di Fisica Nucleare, Sezione di Pisa, Pisa, Italy
AND
M. BARBI
Istituto di Fisica dell'Università, Pisa, Italy

(Received 31 January 1966)

We discuss a numerical method to determine the binding energy and the wave function for a three-body system. Radial wave functions of the form $g_1(r_1)g_2(r_2)g_3(r_3)$ are used, r_1, r_2, and r_3 being the interparticle distances. The method is applied to He^3 and H^3 with central forces and hard core to show the accuracy and the speed of the calculation.

1. INTRODUCTION

THE study of the bound states of three particles is of great interest for molecular, atomic, and nuclear physics. Often only a knowledge of the binding energy is required but sometimes one needs also detailed information about the wave function. The variational method has been extensively applied to these problems with a radial trial function of the form $g_1(r_1)g_2(r_2)g_3(r_3)$, r_1, r_2, and r_3 being the three interparticle distances. Such a radial function is appropriate to describe the correlation between the particles and at the same time has a reasonable asymptotic behavior. The complete wave function is obtained by taking a superposition of products of spin-orbital functions by a radial function of the above type. The disadvantage of the variational analysis is well known. The number of trial parameters and correspondingly the numerical calculations, increase rapidly with the accuracy required for the binding energy and, even more, for the details of the wave function. As an example, when potentials with hard core are considered, trial functions with a great flexibility are necessary to reproduce accurately the exact wave function just outside the hard core, where the potentials have large values. Austern and Iano[1] have proposed a type of trial functions which are constructed with particular attention in the region where the potentials have large values and go over into variational functions for larger distances. Such functions give excellent results for two-particle systems and can be at once extended to the cases of a larger number of particles by choosing the trial function, up to a certain interparticle separation, as a product of the solutions of a two-body Schrödinger equation. This method has been successfully applied[2,3] to particular states of three and

[1] N. Austern and P. Iano, Nucl. Phys. **18**, 672 (1960).
[2] P. H. Wackman and N. Austern, Nucl. Phys. **30**, 529 (1962); E. W. Schmid, Y. C. Tang, and R. C. Herndon, Nuovo Cimento **33**, 259 (1964).
[3] Y. C. Tang, R. C. Herndon, and E. W. Schmid, Nucl. Phys. **65**, 203 (1965); Phys. Rev. **134**, B743 (1964).